Technetium-99m-Labeled Hydrazino Nicotinamide Derivatized Chemotactic Peptide Analogs for Imaging Focal Sites of Bacterial Infection

John W. Babich, Howard Solomon, Marilyn C. Pike, Daniel Kroon, Wendy Graham, Michael J. Abrams, Ronald G. Tompkins, Robert H. Rubin and Alan J. Fischman

Nuclear Medicine Division of the Department of Radiology, the Clinical Investigation and Arthritis Units of the Medical Service and the Surgical Service, Massachusetts General Hospital; and the Shriners Burns Institute, Boston, Massachusetts; the R.W. Johnson Pharmaceutical Research Institute, Raritan, New Jersey; and Johnson Matthey Pharmaceutical Research, West Chester, Pennsylvania

We synthesized and evaluated four hydrazino nicotinamide (HYNIC) derivatized chemotactic peptide analogs: For-NleLFK-HYNIC (HP1), For-MLFK-HYNIC (HP2), For-MLFNH(CH2)6NH-HYNIC (HP3), and For-MLF-(D)-K-HYNIC (HP4), for in vitro bioactivity and receptor binding. The peptides were radiolabeled with ^{99m}Tc via a glucoheptonate co-ligand and their biodistribution determined in rats (n = 6/time point) at 5, 30, 60 and 120 min after injection. Localization of the peptides at sites of deep thigh *Escherichia coli* infection was determined by radioactivity measurements on excised tissues in rats (n = 6/time point) and rabbits as well as scintillation camera imaging in rabbits (n = 6). All peptides maintained biological activity (EC$_{50}$s for O$_2$ production by human PMNs: 12–500 nM) and the ability to bind to the oligopeptide chemoattractant receptor on human PMNs (EC$_{50}$s for binding: 0.12–40 nM). After incubation with ^{99m}Tc-glucoheptonate, radiolabeled peptides were isolated by HPLC at specific activities of >10,000 mCi/μM. Technetium-99m-labeled peptides retained receptor binding with EC$_{50}$s < 10 nM. Blood clearance of all four peptides was rapid. Biodistributions of the individual peptides were similar, with low levels of accumulation in most normal tissues. In rats, all of the peptides concentrated at the infection sites (T/B ratio: 2.5–3:1) within 1 hr of injection. In rabbits, outstanding images of the infection sites were obtained, with T/B ratios of >20:1 at 15 hr after injection. This study demonstrates that ^{99m}Tc-labeled chemotactic peptide analogs are effective agents for the external imaging of focal sites of infection.

J Nucl Med 1993; 34:1964–1974

THe prompt identification, localization and characterization of focal sites of infection is a critical step in the treatment of patients with fever. This is particularly important when localizing symptoms are not present. Although numerous radiopharmaceuticals, including ^{67}Ga-citrate [1], ^{111}In-labeled white blood cells [2] and ^{111}In-labeled IgG [3,4] have been advocated for this purpose, in most cases a delay of 12 and 24 hr between injection and effective imaging is required. This represents a serious deficiency, compared to other imaging modalities (ultrasound, computed tomography or magnetic resonance imaging) which can localize sites of infection much more rapidly.

The time between injection and lesion detection could be significantly reduced by the development of low molecular weight (MW) radiopharmaceuticals that bind to circulating inflammatory cells as well as to cells already present at the inflammation site. Candidate molecules with these characteristics include: IL-8 [5], platelet factor-4 [6] and the peptide, N-formyl-methionyl-leucyl-phenylalanine (For-MLF) [7–9].

For-MLF is a bacterial product that initiates leukocyte chemotaxis by binding to high affinity receptors on the white blood cell membranes [10–12]. These receptors are present on both polymorphonuclear leukocytes (PMNs) and mononuclear phagocytes. Previous studies have demonstrated that many synthetic analogs of For-MLF bind to neutrophils and macrophages with equal or greater affinity compared to the native peptide [6,11,13]. As granulocytes respond to the chemoattractant gradient, the affinity of the receptors decreases as additional receptors are expressed, until the cell reaches the site of inflammation, where the concentration of chemoattractant is greatest [14–16]. Due to the very small size of For-MLF (MW 437), its molecular structure can be readily manipulated to design an optimal imaging agent.

Recently, we demonstrated that ^{111}In-labeled chemotactic peptides are effective agents for the external imaging of focal sites of infection in rats [17]. However, the short biological half-time of the peptides makes ^{111}In a poor choice for imaging. Due to its short physical half-life, high

specific activity, excellent imaging properties, low cost and widespread availability, ^{99m}Tc is the ideal radionuclide for labeling chemotactic peptides. Although numerous techniques have been used for ^{99m}Tc labeling, the hydrazino nicotinamide group has been especially promising. The active ester of hydrazinonicotinic acid (SHNH) has been successfully used to derivatize the epsilon amino groups of lysine residues in proteins. Incubation of these conjugates with simple complexes possessing the Tc(V) oxo core such as ^{99m}Tc-glucoheptonate results in quantitative labeling (18).

The primary objectives of this study were fivefold: (1) synthesize hydrazino nicotinamide (HYNIC) conjugated chemotactic peptide analogs; (2) characterize their receptor binding affinity and agonist properties; (3) characterize the radiochemistry of these analogs; (4) study their biodistribution in normal animals; and (5) study their infection localizing properties in rats and rabbits.

MATERIALS AND METHODS

Peptide Synthesis and Characterization

We synthesized and purified by standard solid-phase techniques (19,20) N-for-norleucyl-leucyl-phenylalanyl-lysine-NH2, N-for-methionyl-leucyl-phenylalanyl-lysine, N-for-methionyl-leucyl-phenylalanyl-diaminohexyl amide and N-for-methionyl-leucyl-phenylalanyl-D-lysine-NH2 as previously described (17). All reagents were obtained as the highest available grade from commercial sources. The nicotinyl hydrazine conjugation of these compounds was performed as described below for HP3.

Dimethylformamide (DMF) (2 ml) and 60 μl of diisopropylethylamine were added to 186 mg of N-For-Met-Leu-Phe-diaminohexyl amide followed by 154 mg succinimidyl-6-t-Boc-hydrazinopyridine-3-carboxylic acid (18) in 1 ml DMF. The mixture became yellow and the peptide dissolved within a short time. After 2 hr, ether-pet ether was added to the reaction mixture and the upper layer was discarded. Water was added to the oily residue causing a solid to form. The solid was washed with 5% sodium bicarbonate, water and ethyl acetate and the yield of crude product was 183 mg. The t-BOC protecting group was removed by stirring the crude product with 5 ml of trifluoroacetic acid (TFA) containing 0.1 ml of p-cresol for 15 min at 20°C. Prolonged treatment with TFA resulted in increased levels of a side product. The TFA was removed by rotary evaporation and ether was added to the residue to precipitate the deprotected peptide. The product was purified by reverse phase HPLC on a 2.5 × 50 cm Whatman ODS-3 column eluted with a gradient of acetonitrile in 0.1% TFA. Fractions containing the major component were combined and the solvent removed to yield the desired product. The peptides For-NleLFK-HYNIC (HP1), For-MLFK-HYNIC (HP2), For-MLFNH(CH$_2$)$_6$NH-HYNIC (HP3) and For-MLF-(D)K-HYNIC (HP4) were characterized by UV and mass spectroscopy as well as amino acid analysis.

Cell Preparation

Human peripheral blood PMNs were isolated by sedimentation in 3% Dextran (Pharmacia, Nutley, NJ) followed by gradient centrifugation on Lymphoprep (Organon Teknika, Durham, NC) as previously described (8,17,21). Cell preparations contained >95% PMN as assessed by light microscopy of Wright stained specimens.

For-MLF Receptor Binding Assay

For-MLF, N-formyl-norleucyl-leucyl-phenylalanyl (For-NleLF) and N-formyl-norleucyl-leucyl-phenylalanyl-norleucyl-tyrosyl-lysine (For-NleLPNleYK) were obtained from Sigma (St. Louis, MO). For-ML[^{3}H]F (60 Ci/mmol) was obtained from New England Nuclear (Boston, MA).

Isolated human PMNs (obtained from healthy volunteers), 8 × 10^5, were incubated in phosphate buffered saline containing 1.7 mM of KH$_2$PO$_4$, 8.0 mM of Na$_2$HPO$_4$, 0.117 M of NaCl, 0.15 mM of CaCl$_2$, 0.5 mM of MgCl$_2$ and 1.0 mM of PMSF pH 7.4 (incubation buffer) at 24°C for 45 min in a total volume of 0.15 ml in the presence and absence of varying concentrations of derivatized peptide and 15 nM of For-ML[^{3}H]F (6,17,22). Following incubation, the cells were filtered onto glass fiber discs (Whatman GF/C; Whatman, Inc., Clifton, NJ) which were then washed with 20 ml of ice-cold incubation buffer. The filters were placed in scintillation vials with 10 ml of Safety-Solve (Research Products International Corp., Mt. Prospect, IL) and radioactivity was measured by liquid scintillation spectroscopy. Specific binding is defined as total binding minus nonspecific binding. Nonspecific binding is the amount of residual bound radioactivity in the presence of 10 μM of unlabeled For-MLF (17,19). Nonspecific binding was approximately 10% of total binding.

To determine the effect of radiolabeling with ^{99m}Tc on binding affinity, isolated human PMNs (2 × 10^6 cells) were incubated in Hank's balanced salt solution (HBSS) (GIBCO, Grand Island, NY) containing 3.4 mM of NaHCO$_3$, 10 mg/ml of bovine serum albumin (BSA) (Sigma, St. Louis, MO), 10 mM of HEPES, pH 7.4 (HBSS/BSA) at 4°C for 60 min in the presence and absence of varying concentrations of For-NleLPNleYK or the corresponding unlabeled peptide and a fixed amount of the ^{99m}Tc-labeled peptide, in a total volume of 0.15 ml. Following incubation, a well mixed aliquot (0.1 ml) of the cell suspension was layered over 0.2 ml of HBSS/BSA:Lymphoprep (1:1) in a 0.4-ml microcentrifuge tube and the contents centrifuged for 4 min at 15,000 rpm (Microfuge E, Beckman, Columbia, MD). The tubes were frozen in liquid nitrogen and the cell pellets were isolated. Radioactivity was measured by gamma counting. Specific binding is defined as total binding minus nonspecific binding. Nonspecific binding is the amount of residual bound radioactivity in the presence of 5 μM unlabeled For-NleLPNleYK or the corresponding unlabeled peptide. Nonspecific binding was approximately 10% of total binding.

Assay of Superoxide Production

Phorbol myristate acetate (PMA) and cytochalasin B were obtained from Sigma (St. Louis, MO). Superoxide release was assayed by monitoring the superoxide dismutase-inhibitable reduction of ferricytochrome C using an extinction coefficient of 29.5/mmol/liter/cm as previously described (17,23). Briefly, isolated human neutrophils were incubated with HBSS alone or with increasing concentrations of peptide (HP1, HP2, HP3, HP4, For-NleLF, For-MLF or For-NleLPNleYK) ranging from 1 nM to 1 μM in the presence of 10 μM of cytochalasin B ± superoxide dismutase (50 μg/ml) at 37°C for 10 min. The reduction of ferricytochrome C was measured spectrophotometrically.

Technetium-99m Labeling of Hynic Derivatized Chemotactic Peptides

Technetium-99m-pertechnetate (^{99}Mo/^{99m}Tc generator) and stannous glucoheptonate (Glucoscan) were obtained from New England Nuclear (Boston, MA). Technetium-99m-glucoheptonate was used to provide the necessary Tc(V) oxo species for radiola-

beling the hydrazinonicotinamide (18) conjugated peptides. Approximately 2.5 ml of ^{99m}Tc-pertechnetate in 0.9% of NaCl was added to the freeze-dried kit. The final radioactive concentration was 5–10 mCi/ml and radiochemical purity of the product was determined by instant thin-layer silica gel chromatography (ITLC-sg) using both acetone and 0.9% NaCl as mobile phase solvents.

The following procedure was used to radiolabel the chemotactic peptide analogs with ^{99m}Tc. Approximately 0.2 mg of peptide was dissolved in 50 μl dimethylsulfoxide and the solution was diluted to a final concentration of 0.1 mg/ml with 0.1 M acetate buffer pH 5.2. Peptide solution (0.5 ml) was placed in a clean glass vial and 0.5 ml of ^{99m}Tc-glucoheptonate was added. The mixture was vortexed briefly and allowed to stand at room temperature for 1 hr. Radiochemical purity was determined by ITLC-sg in three solvent systems: acetone, 0.9% NaCl and acetone and water (9:1).

The ^{99m}Tc-labeled peptide analogs were also analyzed by reverse-phase HPLC using two systems. System A employed a Beckman C_{18} reverse-phase column (5μ, 4.5 × 46 mm, Beckman, Columbia, MD) with the following elution conditions: Solvent A: 5% acetonitrile in 50 mM of acetate (pH 5.2); Solvent B: 50% acetonitrile in 50 mM of acetate (pH 5.2); Gradient: 0% B to 100% B over 20 min; Flow rate 2 ml/min. System B employed a Vydac C_{18} reverse-phase column (300 Å, 5 μ, 4.5 mm × 25 cm, Vydac) with the following elution conditions: Solvent A: 0.1% trifluoroacetic acid in water; Solvent B: 0.1% trifluoroacetic acid in acetonitrile; Gradient: 0% B to 100% B over 10 min; Flow rate 2 ml/min. UV absorption was monitored with a Milton-Roy/LDC flow-through spectrometer and radioactivity was monitored using a Beckman 170 radiation detector (Beckman, Columbia, MD). The outputs from both detectors were recorded and analyzed using a dual channel integrator (Waters Model 746 Data Module, Waters, Marlboro, MA).

Maximization of Specific Activity

To avoid the neutropenic effects associated with pharmacological doses of chemotactic peptide analogs, specific activity of the ^{99m}Tc-labeled chemotactic peptides was maximized so that for an imaging dose of ^{99m}Tc, the final mass of administered peptide is well below the known EC_{50} concentration (~20 nM).

A ^{99}Mo/^{99m}Tc generator was eluted 5 hr after a previous elution in an attempt to minimize the proportion of ^{99}Tc while maintaining a ^{99m}Tc eluant >300 mCi. The mass of the technetium and the relative proportion of ^{99}Tc and ^{99m}Tc were calculated using generator kinetics equations (24) in conjunction with the known history of the ^{99}Mo/^{99m}Tc generator used. Technetium-99m-glucoheptonate (^{99m}Tc-GH) was prepared as described above. Approximately 180 μg of the chemotactic peptide, HP3 (MW: 720), was dissolved in 50 μl of DMSO and diluted to a final concentration of 100 μg/ml with 0.1 M acetate buffer, pH 5.2. Aliquots of the peptide solution were serially diluted with acetate buffer to yield a range of concentrations from 2 to 80 μg/ml. Peptide labeling was initiated by adding 0.5 ml of ^{99m}Tc-GH to an equal volume of peptide in acetate buffer. The solution was vortexed briefly and incubated at room temperature for 1 hr. The extent of peptide labeling was determined by ITLC-sg using three separate solvent systems; acetone, 0.9% NaCl, and acetone and water (9:1). Specific activity of radiolabeled peptide were calculated using the relation: (%RCY × mCi present)/(μmole of peptide × 100).

In Vivo Studies

Three studies were performed in animals: (1) To define the in vivo distribution of the radiolabeled peptide analogs in healthy animals, biodistribution studies were performed with each analog; (2) To determine the ability of radiolabeled peptide analogs to localize at focal sites of inflammation, tissue radioactivity measurements were performed in rats with $E.$ $coli$ infection; and (3) To evaluate the infection imaging properties of the radiolabeled peptides, gamma camera imaging was performed in $E.$ $coli$ infected rabbits.

Biodistribution in Normal Rats

Groups of 24 normal male Sprague-Dawley rats weighing approximately 150 g (Charles River Breeding Laboratories, Burlington, MA) were injected with approximately 5 μCi of each ^{99m}Tc-labeled peptide to determine the biodistribution at 5, 30, 60 and 120 min (each peptide was evaluated in six animals at each time point). Samples of blood, heart, lung, liver, spleen, stomach, kidney, GI tract, skeletal muscle, testes and bone were weighed and radioactivity was measured with a well type gamma counter (LKB Model 1282, Wallac Oy, Finland). To correct for radioactive decay aliquots of the injected doses were counted simultaneously. The results were expressed as percent injected dose per gram (%ID/g) (25).

Studies with Infected Rats

A single clinical isolate of $E.$ $coli$, was employed to produce focal infection. The bacteria were incubated overnight on trypticase soy agar plates at 37°C, and individual colonies were diluted with sterile 0.9% NaCl to produce a turbid suspension containing approximately 2 × 10^9 organisms/ml. Male Sprague-Dawley rats, weighing approximately 150 g (Charles River Breeding Laboratories, Burlington, MA) were anesthetized with ketamine and injected intramuscularly in their left posterior thigh with 0.1 ml of a suspension containing approximately 2 × 10^8 organisms.

Twenty-four hours after bacterial inoculation, animals with gross swelling of the infected thigh were injected with approximately 5 μCi (3 pM) of ^{99m}Tc-labeled peptide via the lateral tail vein. At 30 and 120 min postinjection, groups of five animals were killed by cervical dislocation. Tissue sampling, radioactivity measurements and calculating of results were performed as described above.

Imaging Infected Rabbits

In order to determine the feasibility of using radiolabeled chemotactic peptides for infection localization in animals that are sensitive to the neutropenic effects of these agents, imaging studies were performed in rabbits with focal $E.$ $coli$ infections. A high specific activity ^{99m}Tc-labeled chemotactic peptide was used in these studies. Six male New Zealand white rabbits weighing 2–3 kg were anesthetized with ketamine and xylazine (15.0 and 1.5 mg/kg) and injected in the left posterior thigh muscle with a 1.0-ml suspension of approximately 2 × 10^9 of $E.$ $coli$. Twenty-four hours after inoculation, rabbits with gross swelling in the infected thigh were injected via the lateral ear vein with 600–1000 μCi of HPLC purified ^{99m}Tc-labeled-HP2 (specific activity >10,000 mCi/$\mu$$M$, separated from unlabeled peptide by HPLC as described above). The animals were anesthetized with ketamine and xylazine (15.0 and 1.5 mg/kg) and serial scintigrams were acquired at 0–3 hr and 16–17 hr postinjection using a large field of view gamma camera (Technicare Omega 500, Solon, Ohio) equipped with a high-resolution, parallel-hole collimator and interfaced to a dedicated computer (Technicare 560, Solon, Ohio). Images were recorded for a preset time of 5 min/view with a 15% window centered to include the 140 KeV photopeak of ^{99m}Tc. To characterize the localization of labeled peptide, region-of-interest (ROI) analysis was per-

formed, comparing the infected thigh to the contralateral normal thigh muscle as a function of time.

After acquiring the final images, the animals were killed by pentobarbital overdose and samples of blood, heart, lung, liver, spleen, kidney, stomach, intestine, testes, bone, marrow, normal skeletal muscle, infected skeletal muscle and pus were weighed and radioactivity was measured as described above. To correct for radioactive decay, aliquots of the injected doses were counted simultaneously. The results were expressed as %ID/g. To determine the amount of cell-bound activity in circulation, blood was centrifuged and cells and plasma separated. The cells were washed with 0.9% NaCl and the residual radioactivity in the cells and supernatant measured. To determine the amount of cell-bound activity at the site of infection, the pus was washed twice using 0.9% NaCl and the residual radioactivity in the cellular and soluble fractions was measured.

Statistical Methods

The results of the imaging and biodistribution studies were evaluated by analysis of variance (ANOVA) with a linear model in which organ and time were the classification variables: %ID/g or %ID/organ = Organ + Time + Organ * Time. Post-hoc comparison of peptide concentration was performed by Duncan's new multiple range test (26). The first subscript of each F value is the number of degrees of freedom for: the first classification variable (n − 1), the second classification variable (m − 1) or the interaction ((n − 1) × (m − 1)). The second subscript is the number of residual degrees of freedom (Total number of observations − n × m). All results are expressed as mean ± s.e.m.

RESULTS

Peptide Synthesis

All four HYNIC derivatized chemotactic peptide analogs were prepared in good yield and purity. UV analysis showed maximum absorption at 268 and 315 nm for all four peptides. Mass spectroscopy and amino acid analysis were found to be in agreement with the expected conjugated peptide products.

Biological Activity of Chemotactic Peptide Analogs

The results of the superoxide production assay are shown in Figure 1. The concentrations of peptides which produced 50% of a maximal response (EC_{50}) are given in Table 1. Peptides HP2, HP3 and HP4 had potencies ≥ For-MLF (100 nM). The potency of HP1 was at least an order of magnitude lower. Hence, the order of potency for superoxide production was HP2 > HP3 > HP4 > HP1.

The efficacy of the peptides, defined as the maximal amount of superoxide anion produced, was similar for all peptides tested and ranged from 2.07 to 3.80 moles O_2^- produced/10^6 cells/10 min. The efficacy of all the peptides was less than that of PMA, an unrelated activator of the PMN oxidative burst, which yields a maximal response of 22.9 nmol O_2^- produced/10^6 cells/10 min at a concentration of 0.1 μM.

Binding of Chemotactic Peptide Analogs to Chemoattractant Receptors

Figure 2 shows that the HYNIC derivatized chemotactic peptide analogs inhibit binding of For-ML[^{3}H]F to intact human PMNs with an order of potency similar to that for
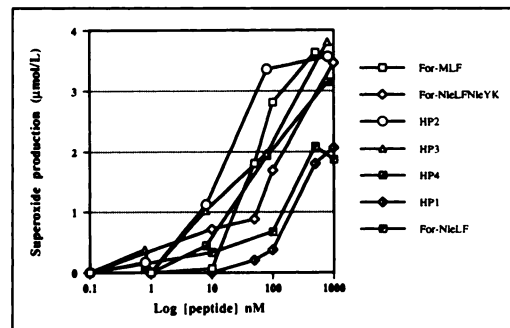

FIGURE 1. Superoxide production by chemotactic peptide analogs. Human PMNs were incubated with HBSS alone or the indicated concentration of peptide for 10 min at 37°C, following which the reduction of ferricytochrome was measured as described in the text.

% of maximal superoxide production = E/M × 100,

where E is the amount of superoxide produced in the presence of an indicated concentration of peptide and M is the maximal amount of superoxide produced by the peptide. For-NleLFK-HYNIC: HP1; For-MLFK-HYNIC: HP2; For-MLFNH(CH₂)₆NH-HYNIC: HP3, For-MLF(D)K-HYNIC: HP4.

production of superoxide anion. The concentrations of peptide required to produce a 50% inhibition of For-ML[^{3}H]F binding to human PMNs (EC_{50}) are given in Table 1. Peptides HP2, HP3 and HP4 had EC_{50} values similar to that of the hexapeptide For-NleLFNleYK. The affinity of HP1 for the chemoattractant receptor while approximately 100-fold lower than the other HYNIC derivatized peptides in this series was only a factor of 2 lower in potency than For-MLF. The tripeptide For-NleLF had over 100-fold lower potency than both the hexapeptide and For-MLF. Hence, the order of affinity for the chemoattractant receptor was HP3 > HP2 > HP4 > HP1. The EC_{50} for ^{99m}Tc-HP2 was <10 nM.

To determine the effect of ^{99m}Tc labeling on receptor binding, the ability of unlabeled HYNIC-peptide to displace ^{99m}Tc-labeled peptides was evaluated using the assay conditions described above. The results of these experiments demonstrated that the concentration of unlabeled peptide required to displace 50% of the neutrophil binding of the ^{99m}Tc-labeled peptide was approximately 10-fold higher than when ForML[^{3}H]F was used as the tracer. This increase in binding avidity could be explained if the radio-

TABLE 1
Maximal Responses (EC_{50}) for Super Oxide Production and Binding Affinity of Chemotactic Peptide Analogs

Peptide	Super oxide production (nM)	Binding affinity (nM)
HP1	500	40
HP2	12	0.18
HP3	40	0.12
HP4	60	0.35
For-MLF	100	20
For-NleLF	320	300
For-NleLFNleYK	100	1

labeled species contains more than one peptide unit per Tc-glucoheptonate and binding is cooperative.

Radiolabeling with Technetium-99m

The Rf values for ^{99m}Tc-labeled peptide and ^{99m}Tc-glucoheptonate on instant thin-layer chromatography-silica gel strips in the solvent systems used to monitor radiolabeling were: 0.9% NaCl-^{99m}Tc-peptide = 0.0, ^{99m}Tc-glucoheptonate = 1.0; acetone-^{99m}Tc-peptide = 1.0, ^{99m}Tc-glucoheptonate = 0.0; and acetone:water (9:1)- ^{99m}Tc-peptide = 1.0 and ^{99m}Tc-glucoheptonate = 0.0. The third system minimized peak trailing, yielding sharper ^{99m}Tc-peptide bands, compared with acetone alone. For all ^{99m}Tc-peptide preparations, ITLC demonstrated that >90% of the radioactivity was associated with the peptide after 1 hr of incubation. Analysis of the labeled peptides using HPLC system A demonstrated major radioactive peaks for ^{99m}Tc-glucoheptonate, ^{99m}Tc-HP1, ^{99m}Tc-HP2, ^{99m}Tc-HP3 and ^{99m}Tc-HP4 with retention times of 0.3–0.5, 14.37, 11.25, 15.11 and 12.96 min, respectively.

Maximization of Specific Activity

The ^{99}Mo/^{99m}Tc generator elution yielded a total activity of 456 mCi. The total amount of technetium was 3.4 nmole with a ^{99}Tc-to-^{99m}Tc ratio of 1.53:1 and the specific activity of the ^{99m}Tc was calculated to be 134,000 mCi/μmole. Technetium-99m-glucoheptonate (^{99m}Tc-GH) was prepared as described above; final radioactive concentration >150 mCi/ml at the time of preparation. Radiochemical purity of ^{99m}Tc-GH was determined to be >95% by instant thin-layer chromatography using both acetone and 0.9% NaCl.

The pharmacological potency of the chemotactic peptide analogs requires high specific activity radiolabeling to reduce the absolute amount of peptide present in the injected solution. Ideally, this level of specific activity should be
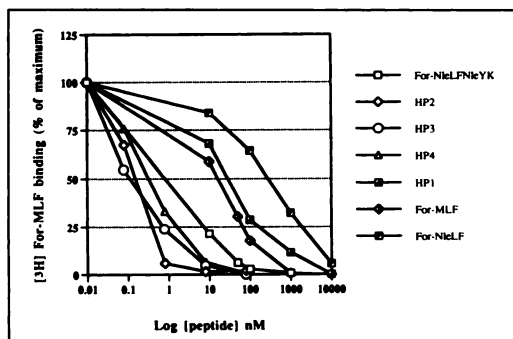

FIGURE 2. Effect of chemotactic peptide analogs on For-ML[3H]F binding to human PMNs. Intact human PMNs (8 × 10^5) were incubated with incubation buffer or the indicated concentration of peptide in the presence of 15 nM For-ML[3H]F for 45 min at 24°C, following which the specific For-ML[3H]F binding was determined.

% of maximal For-ML[3H]F binding=E/C×100,

where E is the specific cpm bound in the presence of the indicated concentration of unlabeled peptide and C is the specific cpm bound of For-ML[3H]F in the presence of buffer alone. For-NleLFK-HYNIC: HP1; For-MLFK-HYNIC: HP2; For-MLFNH(CH2)6NH-HYNIC: HP3, For-MLF(D)K-HYNIC: HP4.
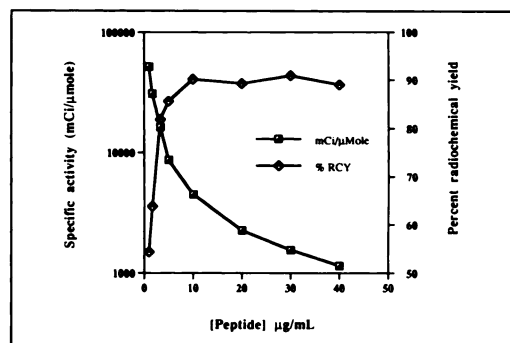

FIGURE 3. Effect of peptide concentration on radiochemical yield (%) and specific activity (mCi/mole). Data is shown for For-MLF(D)K-HYNIC. Similar results were obtained with all peptides tested.

achievable without the need for purification. Figure 3 summarizes the effect of peptide concentration on labeling yield. From this data, it is clear that the final peptide concentration of the reaction mixture has a significant influence on radiochemical yield; at peptide concentrations below 10 μg/ml, poor labeling yields are obtained. When the results are expressed relative to the peptide-to-technetium molar ratio in the reaction mixture, it is apparent that as this ratio increases, the percent of radiochemical yield increases and specific activity decreases.

Using this procedure, it is possible to achieve specific activities of >10,000 mCi/μmole, however, the radiochemical yield decreases substantially below peptide concentrations of 10 μg/ml. At peptide concentrations of <10 μg/ml, a purification step to remove unbound ^{99m}Tc is required. Removal of unreacted ^{99m}Tc glucoheptonate and ^{99m}TcO$_4^-$ can be achieved with reverse-phase Sep-Paks. A further increase in specific activity can be obtained by removing unreacted peptide by HPLC (using System B). Since the peaks corresponding to ^{99m}Tc-labeled peptide, unlabeled peptide and ^{99m}Tc-glucoheptonate are well resolved with this HPLC system, carrier-free radiolabeled peptide can be isolated. Under these circumstances, the specific activity of the radiolabeled peptide is limited only by the specific activity of the eluate from the ^{99m}Tc generator.

Biodistribution Distribution of Technetium-99m Chemotactic Peptides in Normal Rats

The biodistributions of the four ^{99m}Tc-labeled chemotactic peptide analogs are shown in Table 2. In all in vivo experiments, the animals tolerated intravenous administration of the radiolabeled chemotactic peptide analogs without apparent ill effects. With the exception of kidney, stomach and the GI tract, the tissue concentrations of all peptides decreased with time.

In blood, ANOVA demonstrated significant main effects of peptide ($F_{3,70}$ = 56.79, p < 0.0001) and time ($F_{3,70}$ = 252.01, p < 0.0001), however, the peptide by time interaction was not significant. The order of concentrations of the peptides in blood was: HP1 > HP2 > HP3 > HP4 (p < 0.01).

In cardiac tissue, ANOVA showed significant main effects of peptide ($F_{3,64}$ = 44.36, p < 0.0001) and time ($F_{3,64}$

Organ	Time (min)	HP1	HP2	HP3	HP4
Blood	5	1.17 ± 0.070	1.18 ± 0.040	1.01 ± 0.056	0.87 ± 0.046
	30	0.82 ± 0.019	0.67 ± 0.036	0.55 ± 0.017	0.48 ± 0.052
	60	0.67 ± 0.016	0.57 ± 0.033	0.47 ± 0.035	0.36 ± 0.012
	120	0.52 ± 0.010	0.48 ± 0.015	0.39 ± 0.015	0.31 ± 0.010
Heart	5	0.75 ± 0.045	0.50 ± 0.019	0.72 ± 0.089	0.42 ± 0.027
	30	0.50 ± 0.010	0.32 ± 0.016	0.27 ± 0.021	0.22 ± 0.024
	60	0.40 ± 0.012	0.28 ± 0.018	0.29 ± 0.026	0.20 ± 0.013
	120	0.37 ± 0.028	0.26 ± 0.013	0.25 ± 0.024	0.16 ± 0.012
Lung	5	1.54 ± 0.122	0.85 ± 0.043	10.65 ± 1.473	1.11 ± 0.099
	30	0.63 ± 0.043	0.78 ± 0.032	8.45 ± 0.818	0.61 ± 0.071
	60	0.64 ± 0.039	0.46 ± 0.030	5.10 ± 0.449	0.49 ± 0.026
	120	0.46 ± 0.026	0.50 ± 0.025	2.44 ± 0.435	0.37 ± 0.027
Liver	5	0.76 ± 0.056	0.99 ± 0.023	5.72 ± 0.467	0.74 ± 0.091
	30	0.53 ± 0.012	0.62 ± 0.019	4.81 ± 0.205	0.52 ± 0.022
	60	0.45 ± 0.012	0.50 ± 0.022	4.60 ± 0.101	0.51 ± 0.010
	120	0.43 ± 0.016	0.58 ± 0.026	4.75 ± 0.175	0.46 ± 0.016
Spleen	5	0.34 ± 0.014	0.35 ± 0.023	2.27 ± 0.281	0.35 ± 0.041
	30	0.30 ± 0.012	0.39 ± 0.045	2.28 ± 0.231	0.27 ± 0.017
	60	0.26 ± 0.006	0.25 ± 0.013	3.11 ± 0.191	0.32 ± 0.017
	120	0.25 ± 0.007	0.29 ± 0.020	3.01 ± 0.220	0.27 ± 0.009
Kidney	5	3.08 ± 0.092	3.30 ± 0.173	1.90 ± 0.199	3.67 ± 0.436
	30	5.13 ± 0.282	4.82 ± 0.246	1.68 ± 0.064	5.22 ± 0.139
	60	5.16 ± 0.115	4.36 ± 0.213	1.63 ± 0.057	5.36 ± 0.178
	120	5.68 ± 0.143	4.17 ± 0.121	1.60 ± 0.030	4.74 ± 0.201
Stomach	5	0.17 ± 0.024	0.10 ± 0.004	0.38 ± 0.053	0.19 ± 0.011
	30	0.12 ± 0.012	0.15 ± 0.010	0.56 ± 0.029	0.09 ± 0.023
	60	0.15 ± 0.013	0.10 ± 0.005	0.51 ± 0.034	0.15 ± 0.017
	120	0.16 ± 0.015	0.11 ± 0.011	0.39 ± 0.008	0.15 ± 0.012
GI tract	5	0.20 ± 0.013	0.25 ± 0.012	0.33 ± 0.038	0.16 ± 0.005
	30	0.32 ± 0.026	0.64 ± 0.074	0.64 ± 0.046	0.32 ± 0.039
	60	0.23 ± 0.020	0.64 ± 0.089	0.70 ± 0.050	0.39 ± 0.030
	120	0.32 ± 0.028	0.72 ± 0.055	0.81 ± 0.047	0.41 ± 0.035
Testes	5	0.15 ± 0.010	0.12 ± 0.008	0.12 ± 0.011	0.19 ± 0.006
	30	0.14 ± 0.005	0.11 ± 0.003	0.11 ± 0.006	0.14 ± 0.015
	60	0.13 ± 0.005	0.10 ± 0.006	0.11 ± 0.004	0.13 ± 0.008
	120	0.14 ± 0.003	0.10 ± 0.005	0.10 ± 0.005	0.11 ± 0.004
Muscle	5	0.32 ± 0.013	0.25 ± 0.020	0.23 ± 0.015	0.27 ± 0.017
	30	0.22 ± 0.004	0.17 ± 0.018	0.10 ± 0.005	0.17 ± 0.013
	60	0.19 ± 0.008	0.14 ± 0.016	0.12 ± 0.012	0.15 ± 0.009
	120	0.20 ± 0.012	0.15 ± 0.014	0.10 ± 0.007	0.12 ± 0.006
Bone	5	0.55 ± 0.026	0.39 ± 0.011	0.39 ± 0.023	0.37 ± 0.038
	30	0.41 ± 0.009	0.32 ± 0.013	0.26 ± 0.017	0.37 ± 0.019
	60	0.33 ± 0.007	0.30 ± 0.020	0.28 ± 0.023	0.34 ± 0.009
	120	0.32 ± 0.011	0.28 ± 0.012	0.24 ± 0.017	0.28 ± 0.009

*%ID/g (mean ± s.e.m.)

= 98.06, $p < 0.0001$), and a significant peptide by time interaction ($F_{9,64} = 3.69$, $p < 0.001$). The order of concentrations of the peptides was: HP1 > HP3 = HP2 > HP4 ($p < 0.01$).

In lung, ANOVA demonstrated significant main effects of peptide ($F_{3,65} = 183.25$, $p < 0.0001$) and time ($F_{3,65} = 24.56$, $p < 0.0001$), and a significant peptide by time interaction ($F_{9,65} = 13.80$, $p < 0.0001$). The order of concentrations of the peptides was: HP3 > HP1 = HP4 = HP2 ($p < 0.01$).

TABLE 3
Tissue Concentrations of Technetium-99m-Labeled Chemotactic Peptides in Normal and Infected Rat Muscle
(%ID/g tissue ± s.e.m.)

Tissue	Time (min)	Peptide			
		HP1	HP2	HP3	HP4
Normal	30	0.16 ± 0.009	0.11 ± 0.003	0.05 ± 0.009	0.13 ± 0.007
	120	0.10 ± 0.006	0.07 ± 0.004	0.05 ± 0.005	0.13 ± 0.025
Infected	30	0.39 ± 0.013	0.28 ± 0.013	0.11 ± 0.007	0.42 ± 0.049
	120	0.21 ± 0.008	0.16 ± 0.007	0.10 ± 0.004	0.32 ± 0.019

In liver, ANOVA showed significant main effects of peptide ($F_{3,65}$ = 1000.00, p < 0.0001) and time ($F_{3,65}$ = 12.80, p < 0.0001), however the peptide by time interaction was not significant. As in lung, the order of concentrations of the peptides was: HP3 > HP1 = HP4 > HP2 (p < 0.01).

In spleen, ANOVA demonstrated a significant main effect of peptide ($F_{3,63}$ = 431.00, p < 0.0001) and a significant peptide by time interaction ($F_{9,63}$ = 4.64, p < 0.0001). In this organ, the main effect of time was not significant. The order of concentrations of the peptides was: HP3 > HP2 = HP4 = HP1 (p < 0.01). In kidney, ANOVA showed significant main effects of peptide ($F_{3,69}$ = 291.58, p < 0.0001) and time ($F_{3,69}$ = 40.14, p < 0.0001), and a significant peptide by time interaction ($F_{9,69}$ = 10.94, p < 0.0001). The order of concentrations of the peptides was: HP4 = HP1 > HP2 > HP3 (p < 0.01).

In stomach, ANOVA demonstrated significant main effects of peptide ($F_{3,53}$ = 202.98, p < 0.0001) and time ($F_{3,53}$ = 3.10, p < 0.05), and a significant peptide by time interaction ($F_{9,53}$ = 5.56, p < 0.0001). The order of concentrations of the peptides was: HP3 > HP4 = HP1 = HP2 (p < 0.01).

In the GI tract, ANOVA showed significant main effects of peptide ($F_{3,62}$ = 66.30, p < 0.0001) and time ($F_{3,62}$ = 36.32, p < 0.0001), and a significant peptide by time interaction ($F_{9,62}$ = 5.56, p < 0.005). The order of concentrations of the peptides was: HP3 = HP2 > HP4 = HP1 (p < 0.01).

In testis, ANOVA demonstrated significant main effects of peptide ($F_{3,67}$ = 26.97, p < 0.0001) and time ($F_{3,67}$ = 14.94, p < 0.0001), and a significant peptide by time interaction ($F_{9,67}$ = 4.77, p < 0.001). The order of concentrations of the peptides was: HP4 = HP1 > HP3 = HP2 (p < 0.01).

In skeletal muscle, ANOVA showed significant main effects of peptide ($F_{3,59}$ = 48.70, p < 0.0001) and time ($F_{3,59}$ = 97.69, p < 0.0001), however peptide by time interaction was not significant. The order of concentrations of the peptides was: HP1 > HP2 = HP4 > HP3 (p < 0.01). In bone, ANOVA demonstrated significant main effects of peptide ($F_{3,68}$ = 30.15, p < 0.0001) and time ($F_{3,68}$ = 52.84, p < 0.0001), and a significant peptide by time interaction ($F_{3,68}$ = 5.15, p < 0.0001). The order of concentrations of the peptides was: HP1 > HP4 = HP2 = HP3 (p < 0.01).

Localization of Technetium-99m Chemotactic Peptides in Infected Rat Muscle

The tissue concentrations (%ID/g) of the ^{99m}Tc-labeled chemotactic peptide analogs in normal and infected thigh muscle is shown in Table 3. ANOVA demonstrated a significant main effect of peptide ($F_{3,25}$ = 56.51, p < 0.0001), time ($F_{3,25}$ = 59.45, p < 0.0001) and a significant peptide by time interaction ($F_{3,25}$ = 6.74, p < 0.005). In normal muscle, concentrations of HP1 (p < 0.01) and HP2 (p < 0.05) decreased with time while concentrations of HP3 and HP4 remained unchanged. At 30 min after injection, the concentration of HP1 in normal muscle was greater (p < 0.01) than the other peptides and the concentration of HP2 was greater (p < 0.01) than HP3. At 120 min the concentration of HP4 in normal muscle was greater (p < 0.01) than HP2 and HP3; and the concentration of HP1 was greater (p < 0.01) than HP3.

In infected muscle, the concentrations of HP1 (p < 0.01), HP2 (p < 0.01) and HP4 (p < 0.05) decreased with time and the concentration of HP3 (which had the lowest level of accumulation at both times) remained unchanged. At 30 min after injection, the concentrations of HP1 and HP4 were greater (p < 0.01) than the concentrations of HP2 and HP3; and the concentration of HP2 was greater (p < 0.01) than HP3. At 120 min, the concentration of HP4 was greater (p < 0.01) than HP1, HP2 and HP3; and the concentration of HP1 was greater (p < 0.01) than HP3.

The target-to-background (T/B) ratios, (%ID/g infected muscle-to-%ID/g normal muscle), are shown in Figure 4. ANOVA demonstrated a significant main effect of peptide ($F_{3,22}$ = 5.87, p < 0.005). However, the main effect of time and peptide by time interaction were not significant. The T/B ratio for HP4 was significantly greater than for HP2 (p < 0.05), HP1 (p < 0.01) and HP3 (p < 0.01). Thus, HP4 demonstrated not only the highest absolute concentration in infected tissue but also the highest T/B ratios at both times after injection. In contrast, HP3 had both the lowest absolute concentration in infected muscle and the lowest T/B ratio.

Imaging of Focal Sites of Infection in Rabbits

In the rabbit, high levels of ^{99m}Tc-HP4 were detected in the lung, liver and spleen immediately after injection. Lung activity decreased with time and at 1-3 hr after injection,
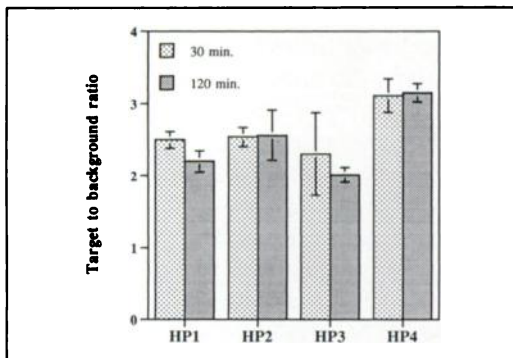
FIGURE 4. Target-to-background ratios for ^{99m}Tc-labeled peptides in rats with *E. coli* infections. The data were calculated by dividing the %ID/g in infected muscle by the corresponding value in contralateral normal muscle. In all cases, infections were established 24 hr prior to injection. Each point is the mean ± s.e.m. for five to six animals.

FIGURE 6. Biodistribution in rabbits with *E. coli* infections of the thigh 17 hr after injection of ^{99m}Tc-labeled HP2. The data are presented as mean %ID/g tissue. Error bars indicate standard error of the mean. The infection was produced 24 hr prior to injection of ^{99m}Tc-HP2.

focal accumulation of radioactivity was observed in the infected thigh. By 4 hr postinjection the T/B ratio was ~4:1. At 16 hr after injection (Fig. 5) the average T/B ratio for the whole lesion increased to 10:1 with focal areas of >20:1. In addition some bowel accumulation was noted at later (>4 hr) time points. The percent residual circulating radioactivity that was cell associated at 16 hr postinjection was determined to be approximately 25%. In contrast, fractionation of the pus demonstrated that approximately 90% of the radioactivity was associated with WBCs.

The tissue concentrations (%ID/g) at 17 hr postinjection, as determined by direct tissue counting, are summarized in Figure 6. The highest concentrations were in spleen > lung > liver = kidney (p < 0.01). The T/B ratios (%ID/g infected muscle or pus-to-%ID/g contralateral normal muscle) are shown in Figure 7. The mean T/B ratios for pus and infected muscle were 25.78:1 (maximum 48.54:1 and minimum 8.84:1) and 14.17:1 (maximum 25.64:1, minimum 4.78:1), respectively.

DISCUSSION

The results of this study demonstrate that HYNIC derivatized chemotactic peptide analogs can be readily labeled with ^{99m}Tc at high specific activity using ^{99m}Tc-glucoheptonate as the source of the Tc(V) oxo core. Furthermore, ^{99m}Tc-labeled peptides are effective agents for the external imaging of focal sites of infection in experimental models of deep thigh infection.

Chemotactic peptides have been the focus of numerous structure-activity studies directed at determining the specific features of the molecule that are responsible for receptor binding and activation (6,27–29). Most of these studies have concentrated on substitutions of natural amino acids in the For-MLF sequence, however, there have been reports of extended peptides and highly negatively charged peptides (17,30) that have EC_{50}s for receptor binding and activation ≤ that of the native peptide. In general, the results of these structure-activity studies have established that although modification at the N-terminus has a profound negative effect on receptor binding and activation, C-terminal modifications have minimal effects

FIGURE 5. Representative gamma camera image of a rabbit with *E. coli* infections of the thigh after injection of a ^{99m}Tc-labeled chemotactic peptide analog. The image was acquired at 17 hr after injection of approximately 1 mCi of ^{99m}Tc-labeled HP2. The infections were produced 24 hr prior to injection.
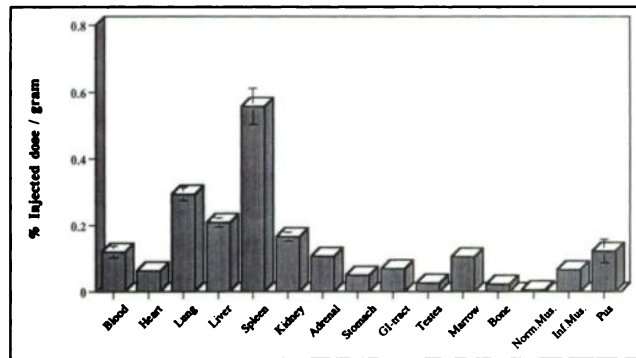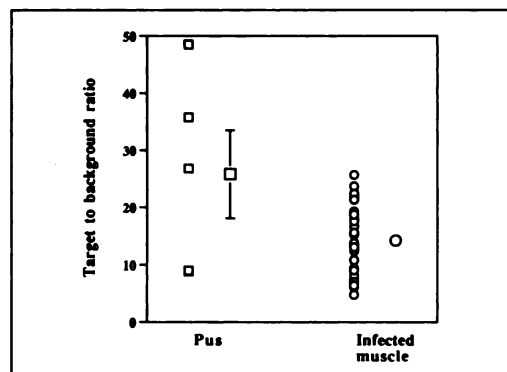

FIGURE 7. Target-to-background ratios for ^{99m}Tc-labeled HP2 in rabbits with *E. coli* infections 17 hr after injection. The data were calculated by dividing the %ID/g in infected muscle or pus by the corresponding value in contralateral normal muscle. In all cases, infections were established 24 hr prior to injection. For infected muscle, the data comprise 28 samples from six animals. For pus, the data are six samples from six animals.

(*31*). In addition, receptor binding and biological activity are highly correlated (*6,8*). Based on these data, a model for the conformation of the receptor-peptide complex has been proposed in which only the N-terminal four amino acid residues interact with the receptor (*32*).

Of the four HYNIC peptides that were synthesized in the present study, three (HP2, HP3 and HP4) had EC_{50}s for receptor binding similar to the hexapeptide, For-NleLFN-leYK, while HP1 was within a factor of 2 of For-MLF. All HYNIC conjugated peptides had an enhanced affinity for the chemoattractant receptor compared to For-MLF. The order of potency for receptor binding was HP3 > HP2 > HP4 > For-NleLFNleYK > For-MLF > HP1 > For-NleLF. Substituting Nle for Met in For-MLF resulted in a 10–15-fold decrease in affinity for receptor binding. However, further derivatization at the C-terminus with -Lys-HYNIC resulted in enhanced receptor binding.

The EC_{50}s for super oxide production of HP2, HP3 and HP4 were enhanced relative to the hexapeptide and For-MLF by 2–8-fold. For-NleLF demonstrated 3-fold lower potency than For-MLF. In contrast to the effect of enhanced receptor binding of HP1 compared with For-NleLF, the EC_{50}s for superoxide production was increased by a factor of 5 compared with For-MLF and For-NleLFNleYK.

When interpreted in light of the proposed model for peptide receptor interaction, these data suggest that HYNIC derivatization at the fourth amino acid residue may result in conformational perturbations that affect both receptor binding and superoxide generation. The most striking observation was the effect of substitution of Nle for Met at position 2 which resulted in >15-fold increase over For-MLF and a 300-fold increase over the hexapeptide in the EC_{50} for receptor binding and a >10-fold increase in the EC_{50} for activation. This result is particularly significant since for previously reported chemotactic peptide analogs, this substitution had minimal effect. The twofold increase in EC_{50} for receptor binding and the fivefold increase in the EC_{50} for activation produced by substitution of D-Lys for L-Lys at position 4 also support this hypothesis. Interestingly, the substitution of 1,6 diamino hexane for L-Lys at this position resulted in only a slight decrease in the EC_{50} for binding and a three- to fourfold increase in the EC_{50} for activation. Labeling the HYNIC conjugated peptides with ^{99m}Tc resulted in an apparent increase in affinity. The results of the ^{99m}Tc-HYNIC-peptide binding assay experiments demonstrated that the concentration of unlabeled peptide required to displace 50% of the neutrophil binding of the ^{99m}Tc peptide was approximately 10-fold higher than when ForML[^3H]F was used as the tracer. This increase in binding avidity could be explained if the radiolabeled species contains more than one peptide unit per Tc-glucoheptonate and binding is cooperative. A similar increase in binding was reported with tetrameric chemotactic peptide analogs (*33*). These results also demonstrate the robustness of the C-terminus toward derivitization.

These observations suggest that in addition to being

excellent radiopharmaceuticals for infection imaging, HYNIC peptides may also serve as model compounds for further elucidating the molecular interaction that accompany the binding of For-MLF to its receptor.

In maximizing the specific activity of HYNIC derivatized chemotactic peptide analogs, we primarily focused on manipulating the source of radionuclide, the eluate of the $^{99}Mo/^{99m}Tc$ radionuclide generator. A potential problem with obtaining high specific activity $^{99m}TcO_4^-$ is the buildup of the long-lived ^{99m}Tc (ground state, $t_{1/2} \sim 10^5$ yr). Since ^{99}Tc is directly produced as a result of 87% of the decays of ^{99}Mo and by 100% of the disintegrations of ^{99m}Tc, there is always some amount of carrier available to compete in the labeling reaction. We have tried to overcome this problem by making frequent elutions of the generator and using the ^{99m}Tc when there is the minimum amount of ^{99}Tc present. With these procedures we demonstrated that ^{99m}Tc-labeled chemotactic peptide analogs with specific activities of >10,000 mCi/μmole can be readily prepared but a Sep-Pak separation of the labeled peptide from other ^{99m}Tc species is required. If in addition to optimizing the source of ^{99m}Tc, the conditions for chromatographic purification of the radiolabeled peptide is also optimized, even higher specific activities can be achieved. With the HPLC system currently in use in our laboratory, the peaks corresponding to ^{99m}Tc-labeled peptide, unlabeled peptide and ^{99m}Tc-glucoheptonate are well resolved and carrier-free radiolabeled peptide can be isolated. Under these circumstances, the specific activity of the radiolabeled peptide is limited only by the specific activity of the ^{99m}Tc generator. Thus, based on the theoretical specific activity of ^{99m}Tc, the maximum specific activity of ^{99m}Tc-labeled HYNIC derivatized chemotactic peptide analogs is approximately 500,000 mCi/μmole. Although achieving this level of specific activity in routine practice is unlikely, it should be possible to prepare radiolabeled peptides with specific activities similar to the ^{99m}Tc-glucoheptonate that is used for labeling. Since we have demonstrated that ^{99m}Tc-glucoheptonate with specific activity of >100,000 mCi/μmole can be prepared on a routine basis, peptides at this level of specific activity should be possible if HPLC purification is employed.

In addition to binding to WBC receptors in vitro, this activity appears to persist in vivo as demonstrated by the significant level of cell-associated radiolabel at the site of infection, and the infection images. In our previous studies with ^{111}In-labeled DTPA derivatized peptides in rats, nearly all of the residual radioactivity in the circulation was cell associated at 2 hr after injection (*17*). In contrast, with ^{99m}Tc-HYNIC peptides at 16–18 hr after injection, only 25% of the radioactivity remaining in the circulation was associated with cells. Since it is unlikely that free peptide persists in the circulation at this time, the residual radioactivity (intact peptide or metabolites) is probably associated with plasma proteins. Although the circulating soluble radioactivity has not as yet been characterized, previous studies with ^{125}I-labeled chemotactic peptide analogs have demonstrated that peptide-receptor complexes are inter-

nalized and degraded by PMNs with release of the radio-label (11). Another difference between the infection imaging properties of ^{111}In-labeled DTPA derivatized peptides in rats and ^{99m}Tc-labeled HYNIC peptides in rabbits is the time course of the decrease in image intensity; the concentration of ^{111}In decreased within a few hours after injection, while the ^{99m}Tc images continued to intensify. Currently, we have no explanation for these differences in lesion kinetics. The rapid clearance of ^{111}In peptides from sites of infection has been considered to be useful for monitoring response to therapy, since, repetitive injections and imaging should not be confounded by residual activity from earlier studies. Due to the short physical half-life of ^{99m}Tc, ^{99m}Tc-HYNIC peptides should be equally useful for this purpose.

A further difference noted between ^{111}In-DTPA peptides and ^{99m}Tc-HYNIC peptides was the higher accumulation in the gastrointestinal tract of the latter. Studies in the rat demonstrate that both For-MLF and For-MLY are rapidly excreted in bile following portal venous infusion in rats or after absorption from the gut lumen (34). Based on these findings it is not surprising that the ^{99m}Tc-labeled peptides exhibit some bowel activity. The difference observed between the ^{111}In-peptides and ^{99m}Tc-peptides is probably related to the metabolic handling of the radiochemical complex and the radionuclide within the liver. Studies focusing on the metabolism of ^{99m}Tc-HYNIC-peptides are underway.

There have been several previous attempts at using radiolabeled chemotactic peptides for infection imaging (17,35–37). However, the radiolabeling methods available at the time of these studies yielded agents of relatively low specific activity, requiring pharmacological amounts of peptide for imaging. These doses of peptide were shown to produce profound transient neutropenia in rabbits (38). With the radiolabeling techniques developed in the present study, these potential adverse effects can be totally eliminated. In rabbits, a species highly sensitive to the neutropenic effects of chemotactic peptides, HPLC purified ^{99m}Tc-HP4 localized at focal sites of E. coli infection within the first hour after injection and reached a maximal T/B ratio at 15 hr.

Our results demonstrate that the HYNIC method of radiolabeling provides a unique and efficient means for preparing ^{99m}Tc-labeled peptides and proteins with extremely high specific activities. The robust nature of the HYNIC method is exemplified by our recent investigations on the preparation of a kit formulation of human polyclonal IgG containing both DTPA- and HYNIC-conjugated protein that can be labeled with either ^{99m}Tc or ^{111}In (39). With this preparation, the presence of millimol-micromole concentrations of Sn(II) resulted in a significant decrease in the efficiency of ^{111}In labeling. In contrast, ^{99m}Tc labeling via ^{99m}Tc-glucoheptonate remained quantitative. These results suggest HYNIC may be uniquely technetium-selective providing a means of direct high specific activity labeling in the presence of metals which interfere with labeling via other chelating agents.

At the high specific activities achieved, it should be possible to perform imaging experiments at peptide concentrations that are significantly below the EC_{50} for the neutropenic response. For example, with SEP-PAK purified peptide (~10,000 mCi/μmole), an injected dose of 20 mCi contains approximately 2 nmoles of peptide. In a 70-kg subject, this represents an injected dose of <30 pmole/kg. Based on previous studies with Rhesus monkeys, this amount of peptide is far below the dose that induces significant neutropenia (unpublished results). With HPLC purified material, the margin of safety should be increased approximately 10-fold. Although, HPLC purification is not convenient for routine clinical practice, we are confident that in the future simpler methods of preparation will be developed.

The results of the in vitro receptor binding studies and the biodistribution data strongly suggest that WBC binding may be a mechanism by which radiolabeled chemotactic peptides localize at sites of infection, however, this has not yet been conclusively proven. If this is a major mechanism of localization, radiolabeled chemotactic peptides should be superior infection imaging agents than radiolabeled autologous WBCs since the peptides can bind to both circulating cells and cells that have previously localized at the site of infection. Another clear advantage over radiolabeled WBCs is the ease of preparation and the fact that blood handling can be eliminated. Although increased vascular permeability could also contribute to infection localization by chemotactic peptides, our previous studies with ^{99m}Tc-DTPA, have demonstrated that this reagent yields T/B ratios of only ~2:1 and the intensity of localization decreases rapidly (definitely within 3 hr). The rapid infection localization by radiolabeled chemotactic peptides has clear advantages over other radionuclide techniques such as ^{67}Ga-citrate, ^{111}In-labeled WBCs and ^{111}In-labeled IgG which typically require 24 hr between injection and imaging and thus are not useful for evaluating acute processes such as appendicitis.

In conclusion, the results of this study establish that HYNIC derivatized chemotactic peptide analogs retain receptor binding and biological activity; are readily labeled with ^{99m}Tc at very high specific activities; and are excellent radiopharmaceuticals for imaging focal sites of infection. The potential advantages of these molecules over current radionuclide techniques for localizing sites of infection are numerous and definitely justify further investigation.

ACKNOWLEDGMENTS

REFERENCES

1. McNeil BJ, Sanders R, Alderson PO, et al. A prospective study of computed tomography, ultrasound and gallium imaging in patients with fever. Radiology 1981;139:647–653.
2. Froelich JW, Swanson D. Imaging of inflammatory processes with labeled cells. Semin Nucl Med 1984;14:128–140.

3. Fischman AJ, Rubin RH, Khaw BA, et al. Detection of acute inflammation with ^{111}In-labeled nonspecific polyclonal IgG. *Semin Nucl Med* 1988;18: 335–344.

4. Rubin RH, Fischman AJ, Callahan RJ, et al. Indium-111-labeled nonspecific immunoglobulin scanning in the detection of focal infection. *N Engl J Med* 1989;321:935–940.

5. Baggiolini M, Walz A, Kunkel SL. Neutrophil-activating peptide-1/interleukin 8, a novel cytokine that activates neutrophils. *J Clin Invest* 1989;84: 1045–1049.

6. Deuel TF, Senior RM, Chang D, et al. Platelet factor 4 is chemoattractant for neutrophils and monocytes. *Proc Natl Acad Sci USA* 1981;78:4584–4587.

7. Showell HJ, Freer JR, Zigmond SH, et al. The structural relations of synthetic peptides as chemotactic factors and inducers of lysosomal enzyme secretion for neutrophils. *J Exp Med* 1976;143:1154–1169.

8. Schiffmann E, Corcoran BA, Wahl SM. Formylmethionyl peptides as chemoattractants for leukocytes. *Proc Natl Acad Sci USA* 1975;72:1059–1062.

9. Williams LT, Snyderman R, Pike MC, Lefkowitz RJ. Specific receptor sites for chemotactic peptides on human polymorphonuclear leukocytes. *Proc Nat Acad Sci USA* 1977;74:1204–1208.

10. Showell HJ, Freer JR, Zigmond SH, et al. The structural relations of synthetic peptides as chemotactic factors and inducers of lysosomal enzyme secretion for neutrophils. *J Exp Med* 1976;143:1154–1169.

11. Schiffmann E, Corcoran BA, Wahl SM. Formylmethionyl peptides as chemoattractants for leukocytes. *Proc Natl Acad Sci USA* 1975;72:1059–1062.

12. Williams LT, Snyderman R, Pike MC, Lefkowitz RJ. Specific receptor sites for chemotactic peptides on human polymorphonuclear leukocytes. *Proc Natl Acad Sci USA* 1977;74:1204–1208.

13. Niedel J, Davis J, Cuatrecasas P. Covalent affinity labeling of the formyl peptide chemotactic receptor. *J Biol Chem* 1980;255:7063–7066.

14. Snyderman R, Verghese MW. Leukocyte activation by chemoattractant receptors: roles of a guanine nucleotide regulatory protein and polyphosphoinositide metabolism. *Rev Infect Dis* 1987;9:S562–S569.

15. Fletcher MP, Seligman BE, Gallin JI. Correlation of human neutrophil secretion, chemoattractant receptor mobilization and enhanced functional capacity. *J Immunol* 1988;128:941–948.

16. Niedel J, Wilkinson S, Cuatrecasas P. Receptor mediated uptake and degradation of ^{125}I-chemotactic peptide by human neutrophils. *J Biol Chem* 1979;10:700–710.

17. Fischman AJ, Pike MC, Kroon D, et al. Imaging of focal sites of bacterial infection in rats with ^{111}In-labeled chemotactic peptide analogs. *J Nucl Med* 1991;32:483–491.

18. Abrams MJ, Juweid M, tenKate CI, et al. Technetium-99m human polyclonal IgG radiolabeled via the hydrazino nicatinamide derivative for imaging focal sites of infection in rats. *J Nucl Med* 1990;31:2022–2028.

19. Merrifield RB. Solid phase peptide synthesis. I. Synthesis of a tetrapeptide. *J Am Chem Soc* 1963;15:2149–2154.

20. Stewart JM, Young JD. *Solid phase peptide synthesis*. San Francisco, CA: W.H. Freeman & Company; 1969.

21. Boyum A. Isolation of mononuclear cells and granulocytes from human blood: isolation of mononuclear cells by one centrifugation and granulocytes by combining centrifugation and sedimentation at 1 g. *Scand J Clin Lab Invest* 1968;21:77–89.

22. Pike MC, Snyderman R. Leukocyte chemoattractant receptors. *Meth Enzymol* 1988;162:236–245.

23. Pike MC, Jakoi L, McPhail LC, Snyderman R. Chemoattractant-mediated stimulation of the respiratory burst in human polymorphonuclear leukocytes may require appearance of protein kinase activity in the cells, particulate fraction. *Blood* 1986;67:909–913.

24. Lamson ML III, Kirschner AS, Hotte CE, Lipsitz EL, Ice RD. Generator-produced TcO$_4^-$: carrier free? *J Nucl Med* 1975;16:639–641.

25. Baker HC, Lindsey RJ, Weisbroth SH. *The laboratory rat*. New York: Academic Press; 1980;257.

26. Duncan DB. Multiple range tests and multiple F-tests. *Biometrics* 1955;11: 1–42.

27. O'Flaherty JT, Showell HJ, Kreutzer DL, Ward PA, Becker EL. Inhibition of in vivo and in vitro neutrophil responses to chemotactic factors by a competitive antagonist. *J Immunol* 1978;120:1326–1332.

28. Rot A, Henderson LE, Copeland TD, Leonard EJ. A series of six ligands for the human formyl peptide receptor: tetrapeptides with high chemotactic potency and efficacy. *Proc Natl Acad Sci USA* 1987;84:7967–7971.

29. Iqbal M, Balaram P, Showell HJ, Freer RJ, Becker EL. Conformationally constrained chemotactic peptide analogs of high biological activity. *FEBS Lett* 1984;165:171–174.

30. Toniolo C, Bonora GM, Showell H, Freer RJ, Becker EL. Structural requirements for formyl homooligopeptide chemoattractants. *Biochem* 1984;23:698–704.

31. Spisani S, Cavalletti T, Gavioli R, Scatturin A, Vertuani G, Traniello S. Response of human neutrophils to formyl-peptide modified at the terminal amino and carboxyl groups. *Inflammation* 1986;10:363–369.

32. Freer RJ, Day AR, Muthukumaraswamy N, Pinon D, Showell HJ, Becker EL. Formly peptide chemoattractants: a model of the receptor in rabbit neutrophils. *Biochem* 1982;21:257–263.

33. Kraus JL, Dipaola A, Belleau B. Cyclo tetrameric clusters of chemotactic peptides as superactive activators of lysozyme release from human neutrophils. *Biochem Biophys Res Commun* 1984;124:945–949.

34. Anderson RB, Butt TJ, Chadwick VS. Hepatobiliary excretion of bacterial formyl methionyl peptides in rat. Structure activity studies. *Dig Dis Sci* 1992;37:248–256.

35. McAfee JG, Subramanian G, Gagne G. Techniques of leukocyte harvesting and labeling: problems and perspectives. *Semin Nucl Med* 1984;14:83–106.

36. Thakur ML, Seifer CL, Madsen MT, McKenney SM, Desai AG, Park CH. Neutrophil labeling: problems and pitfalls. *Semin Nucl Med* 1984;14:107–117.

37. Zogbhi SS, Thakur ML, Gottschalk A, et al. Selective cell labeling: a potential radioactive agent for labeling of human neutrophils. *J Nucl Med* 1981;22:P32.

38. O'Flaherty JT, Showell HJ, Ward PA. Neutropenia induced by systemic injection of chemotactic factors. *J Immunol* 1977;118:1586–1589.

39. Callahan RJ, Wilkinson RA, Babich JW, Fischman AJ. Development of a single radiopharmaceutical kit for radiolabeling human polyclonal IgG with either ^{99m}Tc or [111]In [Abstract]. *J Nucl Med* 1992;33:1024.